INTERFACE

rsif.royalsocietypublishing.org

Research

Cite this article: Hahn EN, Sherman VR, Pissarenko A, Rohrbach SD, Fernandes DJ, Meyers MA. 2017 Nature's technical ceramic: the avian eggshell. *J. R. Soc. Interface* **14**: 20160804.
http://dx.doi.org/10.1098/rsif.2016.0804

Received: 4 October 2016
Accepted: 3 January 2017

Subject Category:
Life Sciences–Engineering interface

Subject Areas:
biomaterials, biomechanics

Keywords:
eggshell, strength, fracture toughness, hoop stress

Author for correspondence:
Marc A. Meyers
e-mail: mameyers@eng.ucsd.edu

Electronic supplementary material is available online at https://dx.doi.org/10.6084/m9.figshare.c.3662806.

THE ROYAL SOCIETY PUBLISHING

Nature's technical ceramic: the avian eggshell

Eric N. Hahn[1], Vincent R. Sherman[1], Andrei Pissarenko[2], Samuel D. Rohrbach[2], Daniel J. Fernandes[4] and Marc A. Meyers[1,2,3]

[1]Materials Science and Engineering Program, [2]Mechanical and Aerospace Engineering Department, and [3]Nanoengineering Department, University of California, San Diego, CA, USA
[4]Biomaterials Laboratory, Military Institute of Engineering, Rio de Janeiro, Brazil

MAM, 0000-0003-1698-5396

Avian eggshells may break easily when impacted at a localized point; however, they exhibit impressive resistance when subjected to a well-distributed compressive load. For example, a common demonstration of material strength is firmly squeezing a chicken egg along its major axis between one's hands without breaking it. This research provides insight into the underlying mechanics by evaluating both macroscopic and microstructural features. Eggs of different size, varying from quail (30 mm) to ostrich (150 mm), are investigated. Compression experiments were conducted along the major axis of the egg using force-distributing rubber cushions between steel plates and the egg. The force at failure increases with egg size, reaching loads upwards of 5000 N for ostrich eggs. The corresponding strength, however, decreases with increasing shell thickness (intimately related to egg size); this is rationalized by a micro-defects model. Failure occurs by axial splitting parallel to the loading direction—the result of hoop tensile stresses due to the applied compressive load. Finite-element analysis is successfully employed to correlate the applied compressive force to tensile breaking strength for the eggs, and the influence of geometric ratio and microstructural heterogeneities on the shell's strength and fracture toughness is established.

1. Background

The function of an eggshell is to protect its contents from mechanical and microbial attack while controlling the exchange of gasses through its porous structure. The strength of an eggshell may be measured as the resistance to impact, puncturing or crushing, and has large repercussions on the ultimate survivability and hatchability of eggs. The eggshell is a multi-layered bioceramic composite comprising a mineral constituent ($CaCO_3$ in the polymorphic form of calcite in most cases [1]) which is intimately associated with an organic matrix [2]. The mineral component is composed of several layers and the prevailing theory is that eggshell thickness is the main variable contributing to the mechanical properties of the shell. There is some evidence that the shell microstructure may also influence mechanical properties [1].

A review of the structure and function of chicken (*Gallus gallus domesticus*) eggshells is given by Hincke *et al*. [3]. The microstructural formation is the result of directed growth exerted by the organic matrix components affecting the size and morphology of growing crystals. The competitive growth process, illustrated in figure 1, results in a columnar microstructure [4–6]. It initiates in the mammillary layer (internal), which is initially composed of discrete aggregations of organic matrix cores surrounded by crystalline material. These cores are suggested as the loci of crystalline formation. There is an observed correlation between the density of this layer and the thickness of the shell which suggests that this layer is intimately related with mineral deposition [4,7]. The mammillary layer lies on top of a thin fibrillar organic membrane that acts as an elastic container for the egg contents.

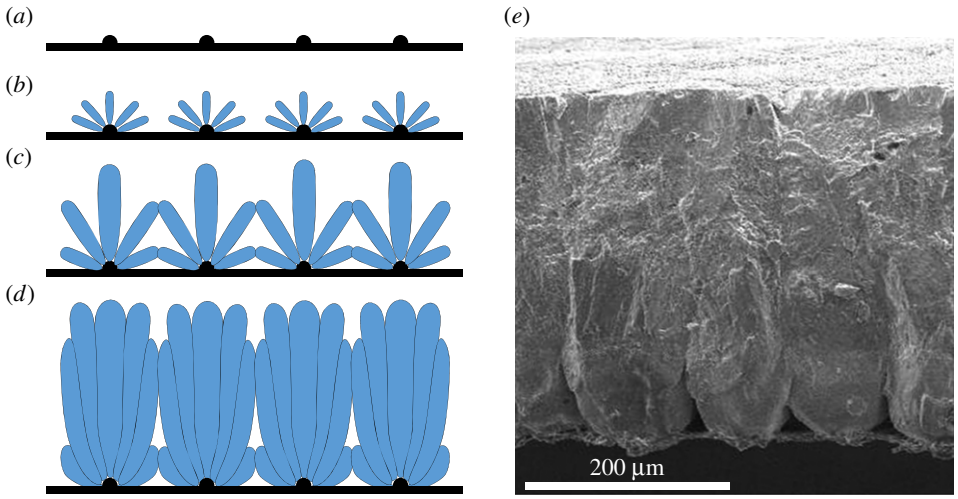

Figure 1. (*a*–*d*) Schematic of the spherulitic growth process that takes place during eggshell formation. Growth initiates at core sites in the mammillary layer (*a*) and develops isotropically as calcite precipitates (*b*). Once lateral advancement is blocked by other neighbouring sites (*c*), the process continues vertically and results in more columnar structures (*d*). (*e*) Scanning electron micrograph of the overall structure of a white chicken eggshell. (Online version in colour.)

The palisades comprise the primary layer and are composed of integrated organic and inorganic components. The organic component accounts for 2–5% of the layer. Crystals, nucleated at discrete points, fan out as columns anchored to the mammillary layer. Upon reaching neighbouring crystals, lateral growth is arrested (figure 1*a*–*d*). Thus, palisade formation is governed by the geometry of the nucleation sites, crystal growth rate and interactions between the growing crystals. From the centre to near the surface, the mineral develops a cross-hatched crystallographic texture. There are also porous channels that extend through the shell up to the cuticle, a protein compound barrier which covers the entire surface. This outer layer is regular and has thickness variation as a consequence of the cracks and flaws which delineate boundaries of the shell pores emanating from the palisades [2,5].

The first well-documented studies of egg shell strength were reviewed in 1961 by Tyler [8] and Tyler & Geake [9]. The United States Department of Agriculture totals the number of 'table eggs' produced in 2015 at 83.1 billion [10]. Of these eggs, it is expected that approximately 6.4% will be damaged or broken between production and reaching the consumer [11,12]. According to the 2015 Consumer Price Index, the average cost for a dozen eggs is $2.47 [13]; this results in an estimated monetary loss of just over 1 billion dollars annually. It is not surprising that within the field of poultry science a significant share of research has been directed towards eggs with the ultimate goal of delivering them to kitchens intact [14–18].

Ar *et al*. [19] evaluated the breaking force of 48 eggshell varieties as a function of weight, finding the force to increase nonlinearly with increasing weight (and thus increasing shell thickness). This and other studies primarily employed flat and rigid plate compression. It has been shown that microfractures at the contact surface significantly reduce the ultimate force at failure [20]. Since the contact area between the plate and the eggshell is small, the loading configuration can be approximated by point loads applied at the poles [20]. With this experimental technique crack initiation is highly localized and the shell fails (at the mammillary layer) [21] after local fracturing of the cap, a mechanism also described as 'polar dimpling' [22]. Other studies of geese (*Anserini*) [23] and ostrich (*Struthio camelus*) eggs [24–26] use compressive testing with flat plates to evaluate the stiffness of larger shells. While the elastic modulus was assessed, the ultimate strength of the eggs was left undetermined and only the breaking force was evaluated. Because the failure is unstable, the accuracy with which the breaking strength can be determined is indeed questionable.

The compression of eggs by flat plates mimics the popularized ring compression test as a means to evaluate brittle tensile failure. The ring test is an extrapolation of the Brazilian disc test, operating under the principal assumptions that the maximum tensile stress occurs on the surface plane along the vertical diametric line, or in simpler terms, the equator. Other adaptations to this test have improved its reproducibility such as the implementation of curved plates or rubber as contacts [27]. This method provides a technique for determining the tensile strength indirectly by evaluating the stress concentration, a factor that increases for a disc with a central hole (a ring) and further increases as the radius of the hole approaches the outer radius. It is straightforward to imagine that the simple stress concentration evaluated in this manner has limitations as the inner radius approaches the outer radius—as in the present case for thin egg shells.

Entwistle & Reddy [28] and Nedomová *et al*. [29] took an alternate approach to study failure by using a hypodermic needle to increase the internal pressure of the egg until fracture. Overall, these studies suggest that the radius of curvature strongly influences the breaking force, adding a layer of complexity to earlier studies which conclude that shell thickness is the primary factor affecting the force at which eggs fail under mechanical loading. Interestingly, two recent studies using Hopkinson split pressure bar have shown that the rupture force is independent of the eggshell curvature during dynamic loading [30,31].

Eggshells resemble structural domes, a predominant architectural design element. The principal applied load includes the weight of the structure and the distributed load from objects the dome supports, such as a bridge and accumulated snowfall. The primary difference between an architectural dome and an eggshell is that the former is anchored at its base such that transverse motion is limited. There exists a dearth of information on tensile failure of

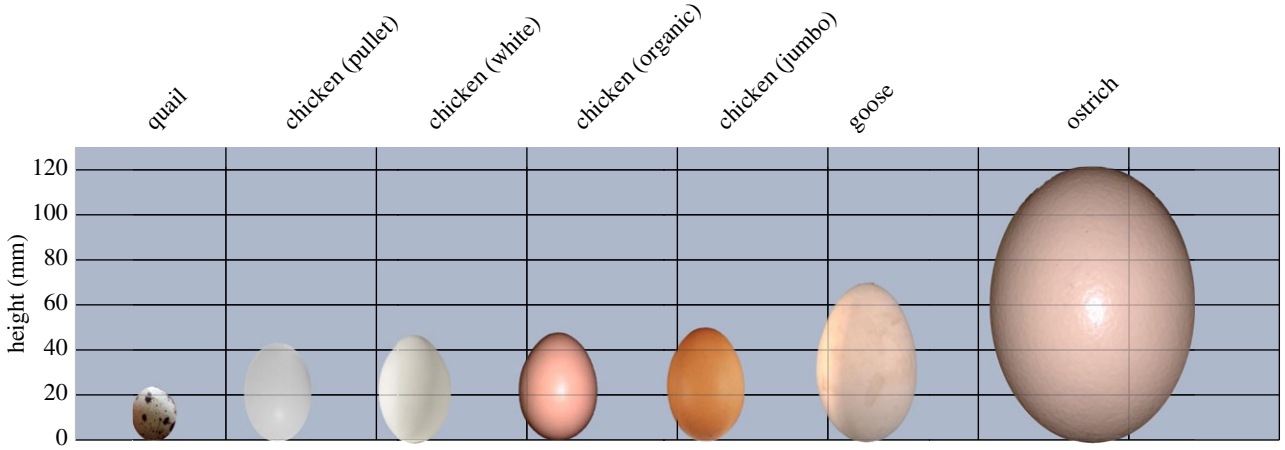

Figure 2. Egg species in order of increasing height/volume: quail, pullet chicken, white-AA chicken, organic-AA chicken, jumbo chicken, goose and ostrich. (Online version in colour.)

hollow spheres under compressive loads. The present research may provide unique insights into the failure of architectural structures, porous granular solids and foams through the study of a structure tailored by nature: the avian eggshell. Furthermore, the applicability of allometric scaling laws in nature is questioned: eggs from different species and thus sizes were tested. Answers are provided on whether the size ratio dictates their mechanical properties.

2. Material and methods

2.1. Egg specimens

Eggshells from several bird species were obtained from multiple vendors. Jumbo chicken eggs were obtained from Hilliker's Ranch Fresh Eggs in Lakeside, CA, USA. Chicken, pullet chicken, goose and quail (*Coturnix coturnix*) eggs were obtained from local farmers' market vendors in La Jolla and Escondido, CA, USA. Ostrich eggs were obtained from OstrichLand USA in Buellton, CA, USA. AA organic and regular chicken eggs were also obtained from the local supermarket. Figure 2 shows scale comparison of the sizes of these eggs.

Prior to mechanical testing, measurements of the long and short axes were taken with Mitutoyo calipers with an accuracy of ± 0.02 mm and a resolution of 0.01 mm. Measurements of eggshell thickness were taken at the blunt end of the egg after fracture. This portion of the egg was consistently recoverable and has a low degree of curvature, reducing error in measurement. Prior studies [32,33] indicate that the global variation of eggshell thicknesses is small.

2.2. Mechanical testing

An Instron 3140 equipped with a 30 kN load cell was used to compress eggs along their major axis in the two shown loading configurations: figure 3*a*, with rubber pads to distribute the load around the pole of the egg; and figure 3*b*, with no cushion such that point loading occurs at the poles. The load cell is calibrated and balanced using Instron's Bluehill 3 software. The major axis is loaded because symmetry along it is greater than along the minor axis, and this improves our ability to use an ellipsoidal model to compare the deformation using finite-element analysis (FEA).

In the loading configuration shown in figure 3*a*, the rubber distributes the load across the surface of the egg and maintains a predetermined contact angle as will be discussed in greater detail in the following sections. A nominal strain rate of $10^{-3}\,\mathrm{s}^{-1}$ was applied, as determined from the speed of the

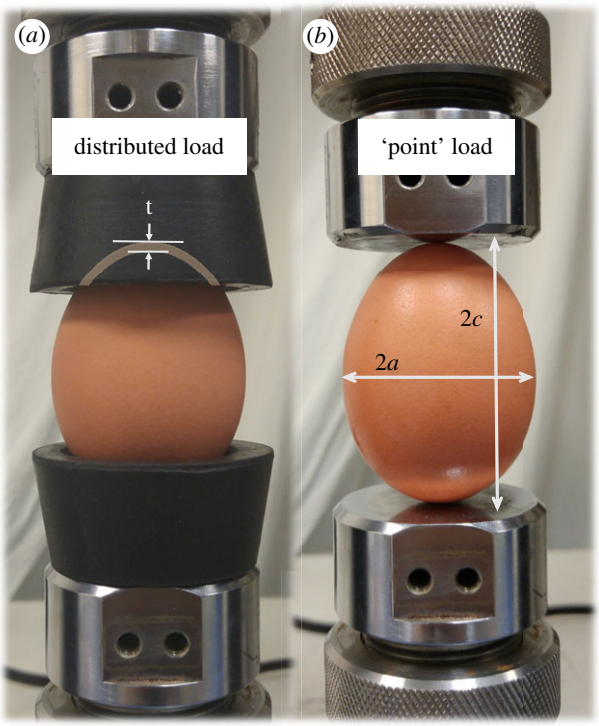

Figure 3. Mechanical testing fixture with organic chicken egg specimen. (*a*) Distributed load configuration: the applied normal load is transferred to the egg through rubber pads with a spherical cut removed from the centre. This increases the load distribution and also reduces sliding/slipping during the experiment. (*b*) Point load configuration. (Online version in colour.)

cross head and the length of the major egg axis. In reality, the strain rate is lower due to the compressibility of the rubber cushions. Previous evaluations of the strain-rate sensitivity by Voisey & Hunt [34] showed that loading velocities of $20\,\mathrm{cm\,min}^{-1}$ (estimated approximately $5.7 \times 10^{-2}\,\mathrm{s}^{-1}$) or lower minimize the effects of strain-rate sensitivity in chicken eggs. The experiment was imaged using a Phantom v.120 capturing 18 000 frames per second at a resolution of 512×512, and the scale of the images is calibrated using a known measurement (the diameter of the egg measured using the above-mentioned calipers) at the focal plane, which can be adjusted by the lens system. Owing to the rapid failure, the eggs were tested inside plastic bags to contain the broken shell and fluid. We refer to tests conducted with rubber as distributed load experiments.

In order to determine the effect the inner fluid of the egg has on the strength of an egg, a set of white-AA chicken eggs were

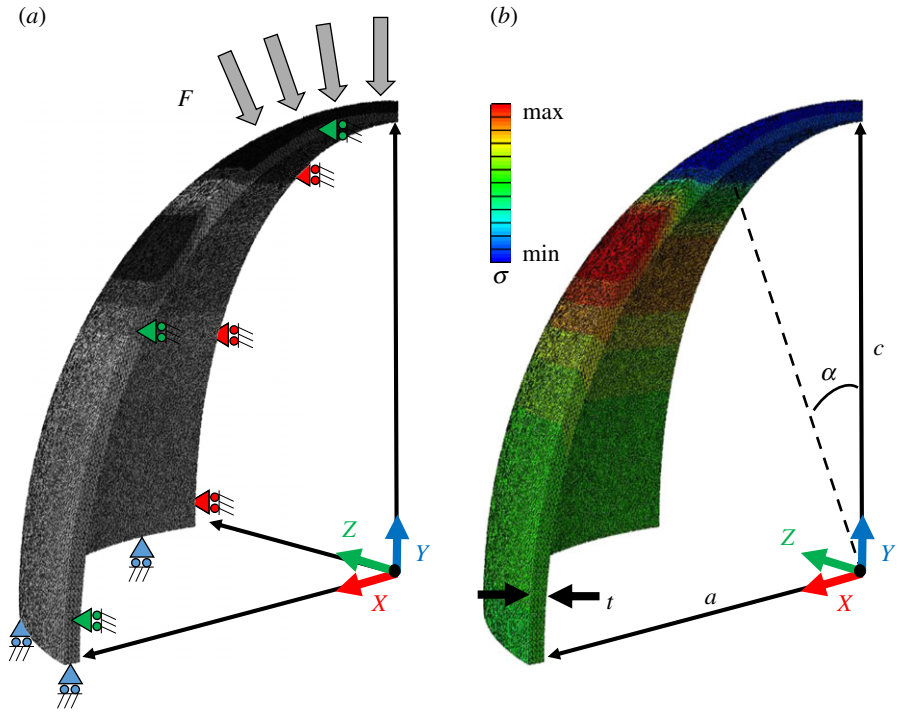

Figure 4. Finite-element analysis of maximum principal stress as a function of egg shape, thickness and loading area. (*a*) Boundary conditions are indicated at symmetry planes of the eggshell. Each colour is associated with a given direction of symmetry based on the coordinate system indicated on the figure. (*b*) The highest tensile stresses are located below the loading area of the egg. (Online version in colour.)

hollowed and tested in an equivalent scheme. A small hole was first drilled in the top of each egg. Each egg was then inverted and exposed to vacuum to empty the contents. This set of hollow eggs was tested against a control set of identical white-AA chicken eggs.

Chicken eggs were also compressed to failure between parallel flat metal plates to replicate the deformation and failure mechanisms observed by Macleod *et al*. [20]. As in the tests with the rubber cushions, the major axis of the eggs was aligned with the direction of compression. Two sets of eggs were compressed at strain rates ($\dot{\varepsilon}$) of 1.5×10^{-3} s^{-1} and 1.5×10^{-6} s^{-1}. A stop condition of 90% maximum force drop was enforced to prevent complete fracture. The first set ($\dot{\varepsilon} = 1.5 \times 10^{-3}$ s^{-1}) approximately replicated the rate used by Macleod [20], 5 mm min^{-1} applied to chicken eggs approximately 55 mm tall. The second set ($\dot{\varepsilon} = 1.5 \times 10^{-6}$ s^{-1}) was tested with an extension rate of 50 µm min^{-1}. We refer to tests conducted with plates as point load experiments.

2.3. Finite-element analysis

The FEA of both loading configurations allows for a more accurate evaluation of stress concentration and deformation for varying macroscopic egg parameters and applied forces. Models were generated with the aid of the commercially available FEA modelling software ABAQUS CAE v. 6.12.

Dimensions taken from tested eggshells (radius a, half-height c and thickness t) were used to model the geometry. Eggshells were modelled here as hollow spheroidal shells made out of a linear-elastic homogeneous-isotropic material. The layered structure of the eggshell, as described in §1, was not taken into account because the elastic deformation is primarily a function of the stiffness of the mineral properties, and not the thin underlying membrane or the outer cuticle. This is a simplification of the inhomogeneous and anisotropic egg shell structure that allows for a solution with a reduced number of variables, and provides an appropriate estimation of the global behaviour of the shell in compression. We assume that the shell deforms elastically until the nucleation of the first crack, after which brittle failure occurs. Therefore, FEA is limited to the elastic regime and is used to determine the relationship between the macro-geometry and applied load. Although the highly mineralized shell exhibits brittle failure, a corresponding failure model is not necessary as only the appearance of the first crack is studied and not its propagation. We hypothesize that the crack forms when the principal maximal stress reaches the failure strength of the material. Using the model, the principal maximal stress for a given load can be calculated and thus failure strength can be estimated.

To reduce computation time, only one-eighth of an eggshell was represented by taking advantage of the structural symmetries (figure 4). Adapted boundary conditions were applied on symmetry planes. In both cases, three-dimensional tetrahedral quadratic elements (C3D10) mesh the structure, with a minimum of four elements through the thickness to avoid locking (and an apparent increase in bending stiffness). An adaptive meshing rule ensures the convergence of the computation within a 5% margin of error in terms of stresses. Three-dimensional continuum elements were preferred to shell elements in order to distinguish and visualize stresses throughout the eggshell thickness and minimize problems related to surface bending due to a discontinuity at the edge of the applied load (i.e. the load transitions instantaneously from the applied value to zero).

For the point load experiment, an analytical rigid plate representing the plate displaces towards the cap of the shell and the resulting reaction force is then measured to match it with experimental data. A hard frictionless contact models the interaction between the two solids. Distributed load experiments were simulated by applying a uniformly distributed normal pressure over a surface portion of the cap, defined by an angle $\alpha = 30°$. The total magnitude of the applied load equals the experimental breaking force for each egg.

3. Results and discussion

3.1. Compression tests

Representative force versus displacement curves are given for the distributed load (figure 5) and point load (figure 6)

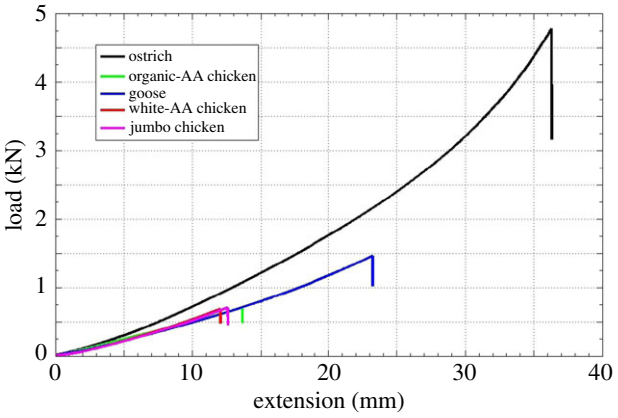

Figure 5. Representative force versus extension curve for various eggshells loaded with rubber cushions (distributed load geometry). (Online version in colour.)

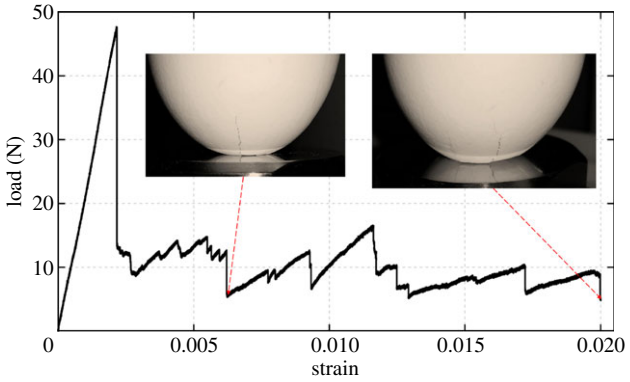

Figure 6. Representative force versus extension curve for regular chicken egg loaded without rubber cushion at 5 mm min^{-1}, $\dot{\varepsilon} = 1.5 \times 10^{-3}$ s^{-1} (point load geometry). (Online version in colour.)

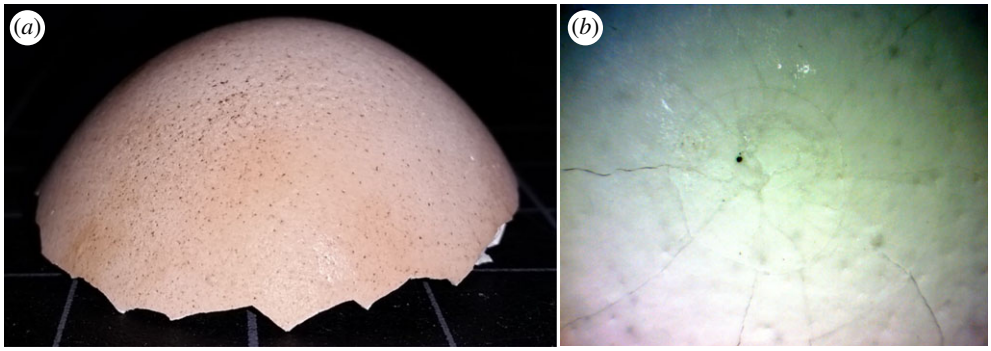

Figure 7. (*a*) Intact egg cap resulting from distributed load experiment. (*b*) Local fracturing/cracking failure resulting from point load experiment. (Online version in colour.)

configurations. For flat plate point load tests, our findings align with those of previous researchers [20]. Failure by stresses at the caps causes the shell of the egg to crack locally, but a resulting increase in contact area provides stress relief and limits the growth of the initial cracks. The experimental set-up has a stop condition of 90% load drop and the membrane fully survives. Figure 6 shows a top projection highlighting the local failure of a chicken egg subjected to a pseudo-point load. Here pseudo refers to the fact that as the egg shell fails, the contact area is increased. Local failure and crack suppression by stress release can be identified at the load drops seen in figure 5.

The failure for the distributed load configuration is confined to the shell that is not in contact with the rubber. Figure 7 presents an image of a preserved egg cap recovered from a distributed load test. An interesting breaking mechanism is indeed observed as a first crack appears at a certain offset from one of the rubber pads and propagates vertically. Then, additional evenly spaced vertical cracks form around the egg and the resulting strips fracture horizontally. This process has been observed in detail by high-speed imaging of the compression tests for chicken, goose and ostrich eggs and is illustrated in figure 8 for the latter. The electronic supplementary material contains videos of failure. The measured velocity of the first vertical crack in ostrich eggs is 610 ± 40 m s^{-1}.

The breaking forces with the distributed load configuration of all tested egg types are presented figure 9 and appear to show a linear relationship with eggshell radius, chosen here as a representative parameter for egg size. This obtained data are further used to estimate failure strength.

3.2. Determining failure strength

The appearance of vertical cracks during distributed load tests confirms that failure occurs due to tensile hoop stresses in the distributed loading configuration. The eggshells' failure strength was estimated analytically and fed into experimental parameters for FEA. The eggshells are assumed to be prolate spheroids with radius a and half-height c ($c > a$). We make a first order approximation that eggshells can be represented as homogeneous-isotropic linear-elastic materials with a Poisson ratio of 0.3. We hypothesize that failure occurs at the location of maximum tensile stress.

For the distributed load experiments with rubber pads, we consider the vertical load applied by the Instron to be fully transferred via the pads to the shell. The result is a uniformly distributed normal pressure over the surface of the shell delineated by a cone of opening angle 2α.

In order to determine the failure strength, the maximum value of the hoop stress $\sigma_{\theta\theta}$ is determined at the measured breaking force F. Membrane theory [35] is applied in order to determine the stress resultant, N_θ, which is defined as a force per unit length:

$$N_\theta = \frac{1}{2\pi r_1 \sin^2\phi} \int_0^\phi p_r \cos\phi \, (2\pi r_0) r_1 \, \mathrm{d}\phi \tag{3.1}$$

and

$$N_\theta = \int_{-t/2}^{t/2} \sigma_{\theta\theta} \, \mathrm{d}r, \tag{3.2}$$

where $r_1 = \mathrm{d}r_0/\cos\phi \, \mathrm{d}\phi$ is the local radius of curvature of an infinitesimal portion of the membrane, r_0 is the projection of

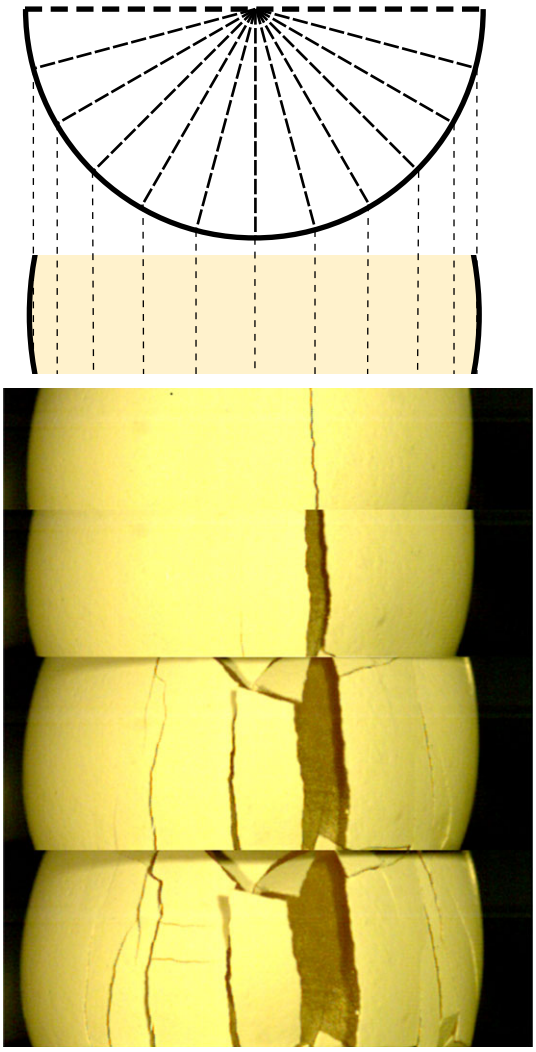

Figure 8. Vertical crack spacing during dynamic fracture. The high-speed photography captures a projection which is related to a radial spacing through the projection shown above. (Online version in colour.)

the mean radius on the axis of revolution, ϕ is the latitude and t is the shell thickness. The normal pressure p_r corresponds to the force F divided by the surface S of the cap on which it is being applied.

Finally, an approximated expression of $\sigma_{\theta\theta}$ is obtained by neglecting its variation throughout the thickness:

$$\sigma_{\theta\theta} = \frac{N_\theta}{t} = \frac{N_\theta}{R_{\text{ext}}(1-\rho)}. \tag{3.3}$$

Both membrane theory and FEA can be used to predict the maximum tensile stress based on geometric parameters and breaking force. For the sake of simplicity, the example of hollow spherical shells ($r_1 = r$, $r_0 = r\sin\phi$; $r = R_{\text{ext}} - t/12$) under uniform axisymmetric loads over a portion of the caps delimited by a cone of half-angle $\alpha = 30^\circ$ is provided here.

Membrane theory yields the following equation for the hoop resultant:

$$\left.\begin{aligned} N_\theta &= -\frac{p_r}{2} \quad \text{if } 0 \le \phi \le \alpha \\ \text{and} \qquad N_\theta &= \frac{p_r \sin^2\alpha}{2\sin^2\phi} \quad \text{if } \alpha < \phi \le \frac{\pi}{2}, \end{aligned}\right\} \tag{3.4}$$

with $p = F/S$ and $S = 2\pi R_{\text{ext}}^2(1-\cos\alpha)$.

Figure 10 presents the calculated hoop stresses as a function of the latitude angle, φ, for spheres of varying thicknesses (with thickness to radius ratios comparable with experimental values measured for different types of eggshells) estimated with both membrane theory and FEA. Owing to the discontinuity in load, the analytical approach results in a piecewise function defining the hoop stresses (see equations (3.3)–(3.4)). Although estimated stresses have comparable values away from the discontinuity, the analytical method overestimates the maximum tensile stress and places it at the edge of the applied load. FEA show that stresses are continuous due to local bending of the shell and the maximum value is obtained at a few degrees away from the loaded region, as seen during testing of eggs.

Bending moments occurring in thin shells of revolution undergoing localized loads have been extensively discussed in the literature [35,36] and calculating them can become very intricate. It also introduces additional variables in the analytical expression of the hoop stresses, such as the Poisson ratio, which has a notable influence on the estimated value. Thus, the FEA is recommended to palliate this problem.

The finite-element model (figure 4) was, therefore, preferred to calculate the maximum stress using measured experimental values of the radius, half-height, thickness, contact angle α (kept constant at 30°), and an assumed Poisson ratio of 0.3. As shown by Reissner [37], no influence of the Young's modulus, E, is observed for the determination of the stresses; it was therefore kept constant at 10 GPa.

Figure 11 presents the results obtained in this fashion. They suggest a trend of decrease in strength as eggs increase in size, ranging from 30.9 MPa for pullet chicken eggs down to 8.5 MPa for ostrich eggs. Binning data by thickness (0.05 mm bin size) the power regression is calculated, obtaining a relationship of $\sigma_{\max} = 14.38t^{-0.55}$ with $r^2 = 0.95$. Quail eggs (25.6 MPa) appear to be an exception to this trend, which may be due to differences in the cuticle layer and an apparent increase of porosity. The strength values are in reasonable agreement with what has been observed for limestone (primarily composed of calcite) and reported by Fuenkajorn *et al.* [38], where mean strengths of 10.9 MPa for the Brazilian test and 23.2 MPa for the ring tensile test were obtained.

Interestingly, simulations of point load tests indicate that such stresses are reached much earlier during compression, yet often no crack initiation is observed under the cap. The shell yields when a sufficient portion of the cap is deflected and circumferential cracks form around this region. This is consistent with observations made by ourselves and Macleod *et al*. [20]. An explanation for this can be imputed due to the symmetry of revolution of the structure which prevents cracks from forming and propagating along their axis of symmetry. As a result, assessments of failure strength based on point load type experiments can potentially lead to erroneous values when referring to force–displacement curves.

3.3. Weibull analysis

Testing of hollowed (interior fluid removed) chicken eggs and comparing them to the whole chicken eggs showed no significant difference in strength or failure distribution based on a Scheffé analysis (Scheffé $p = 0.65$). This indicates that the fluid inside the egg neither adds nor subtracts from the structural strength of the eggshell; this is likely, in part, due

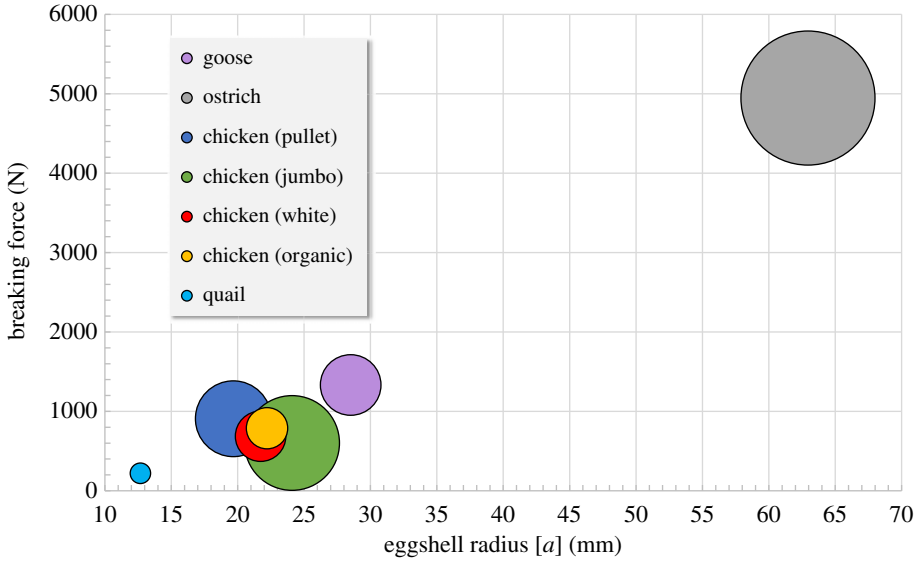

Figure 9. Normal force at failure as a function of eggshell radius. Each circle is centred on the mean breaking force and the radius is proportional to the standard deviation for each given type of egg. The force increases with egg size. (Online version in colour.)

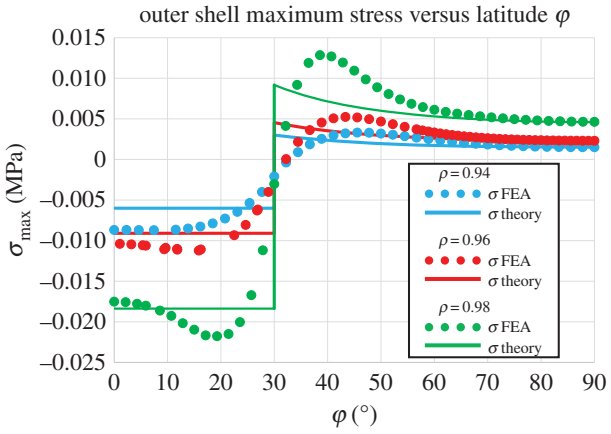

Figure 10. Variation of the maximum stresses according to latitude φ on the outer layer of a spherical shell of radius $r = 30$ mm and varying thickness ratio ρ for a force of 100 N applied over a contact surface defined by an angle of 30°. Membrane theory and FEA results are compared and show that bending moments occurring at the discontinuity affect the value and location of the maximal stresses. (Online version in colour.)

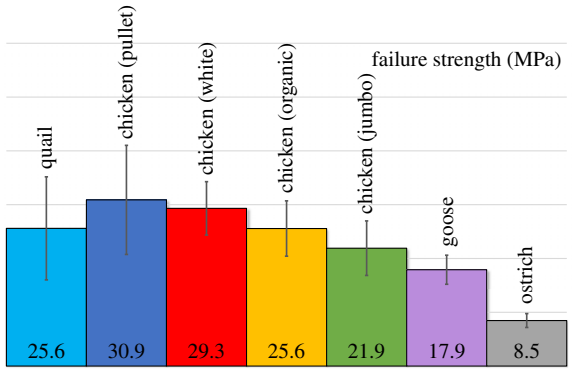

Figure 11. Average tensile failure stress for the different types of eggs. Results are ordered by egg size and error bars represent the standard deviation for each type. Despite the particular case of quail eggs, failure strength decreases as the egg size increases. (Online version in colour.)

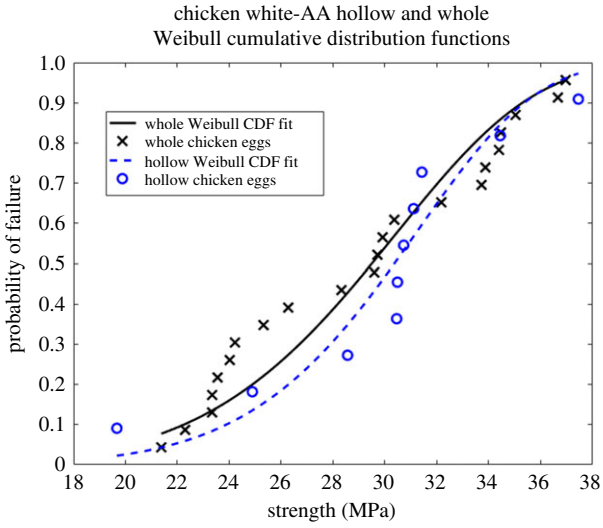

Figure 12. Weibull cumulative distribution functions (CDF) of whole and hollow (fluids removed) white-AA chicken eggs. (Online version in colour.)

to a compressible air sac within the egg. Thus, this claim enables us to justify neglecting internal fluids during FEA.

Weibull distributions are used for strength analysis because of the brittle nature of eggshells as well as the natural variability of biological materials. The failure probability (F) at a given stress (σ) for a brittle material is

$$F = 1 - \exp\left[-\left(\frac{\sigma}{\sigma_0}\right)^m\right], \tag{3.5}$$

where σ_0 is the characteristic strength and m is the Weibull modulus. The Weibull modulus is a measure of how reliable a material is. A high value indicates that there is low variance from the characteristic strength. Typical Weibull moduli for traditional ceramics such as clay or rock are typically below 3, and engineered 'technical' ceramics are defined by a Weibull modulus in the range of 5–10 [39]. Figure 12 shows the results of the Weibull analysis of hollow and whole eggs; the Weibull moduli are 8.9 and 7.3, respectively, and thus eggshells qualify as a 'technical' ceramic.

Our assumptions thus far have treated the eggshell as a homogeneous and isotropic. If this were truly the case, scaling the egg would have no effect on strength as long as the curvature and relative thickness of the egg remained

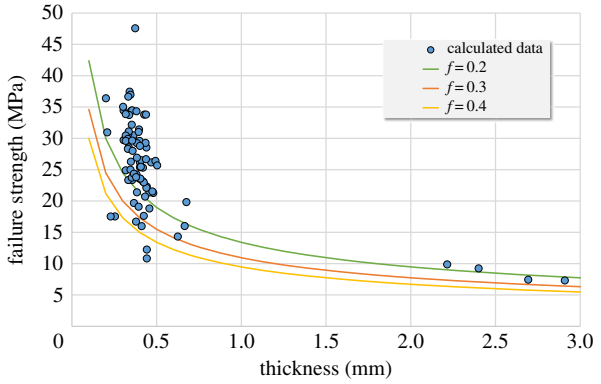

Figure 13. Tensile failure strengths (circles) computed by FEA, as a function of shell thickness, are compared with failure induced by fracture toughness (solid lines) for varying values of *f*, a dimensionless factor representing the fraction of the shell with pre-existing cracks along the thickness. (Online version in colour.)

constant. Our analysis, although limited to the pre-stated assumptions, has identified that the strength of the eggshells is not entirely dictated by its geometry/size. This is despite the fact that force at failure increases with egg size (and thus shell thickness), a trend that relates primarily to the dimensional relationship between force and stress.

3.4. Influence of microstructural flaws on failure strength

The tensile strengths show, with the exception of the quail eggs, a gradual decrease with increasing size. This can be rationalized in terms of pre-existing microstructural flaws, which are observed principally in the larger eggs. The 'palisade' portion with parallel calcium carbonate crystals occupies a fraction between 0.2 and 0.4 of the egg thickness. It is easy to envisage imperfect bonding at the interface between adjacent spherulitic nucleation and growth sites, as shown in the sequence of figure 1. Application of fracture mechanics can yield a dependence of σ_{max} on a_c, the crack size (for a surface penny-shaped geometry):

$$K_c = Y\sigma_{max}\sqrt{\pi a_c}, \tag{3.6}$$

where K_c is the fracture toughness. For the geometry closely resembling the one in eggs, one can approximate $Y \sim 1.12$. A recent study by Taylor *et al.* [40] reports $K_c \sim 0.3\ \mathrm{MPa}\sqrt{m}$ for chicken eggs. By setting $a_c = ft$, with t being the eggshell thickness we can estimate a portion of it, f, that is pre-cracked. As defined, $f < 1$. Thus, the experimental results are compared with the predictions of equation (3.6) for three values of f: 0.2, 0.3 and 0.4. It can be seen that fracture mechanics predicts results that are compatible with our data (figure 13). The $t^{-0.55}$ in the fit from §3.2 ($\sigma_{max} = 14.38t^{-0.55}$) shows close agreement with this micro-defects model that has a $t^{-0.5}$ relationship with strength. It should also be mentioned that porosity, not directly considered here, can affect the strength.

There are also intrinsic differences between eggs of different species related to diet and other sources. Micrographs presented in figure 14 reveal that the cuticle of the quail egg is significantly more defined and tortuous than other eggshells (white chicken and ostrich), resembling dried and cracked mud. Therefore, a plausible explanation for the lower strength of the quail egg is the abundance of these pre-existing crack nucleation sites.

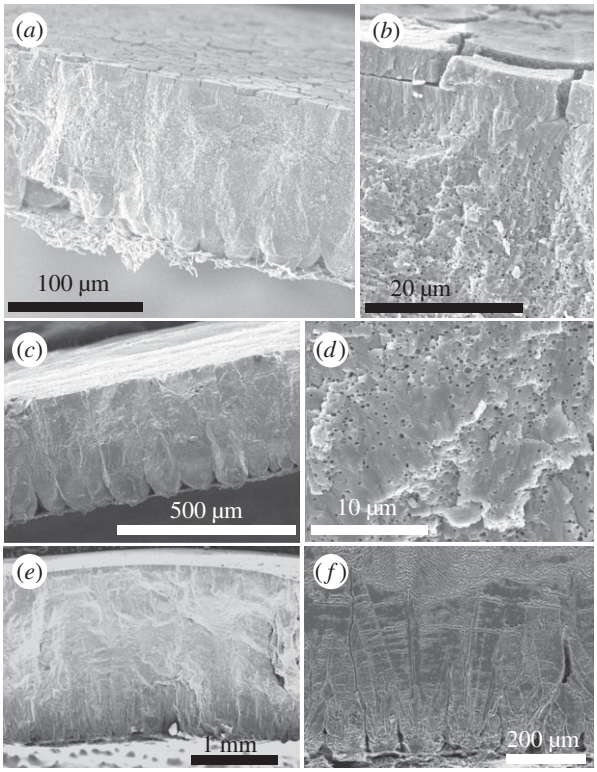

Figure 14. Scanning electron microscopy images of cross-sections of a quail (*a*,*b*), a white chicken (*c*,*d*) and an ostrich (*e*,*f*) eggshells. Characteristic spherulitic structures formed in the mammillary region of the shell lie between a thin fibrous organic membrane near the inner layer and a denser and compact region called the palisades. A thin cuticle forms the outermost layer. Varying palisade heights, spacing and porosities can be observed among egg types.

The decay of strength with increasing size can also be explained by a stochastic micro-defects model. It appears that the density of defects is relatively constant, and therefore, the larger shells contain a much greater total quantity of defects. A solution for defect dominated failure has been evaluated for a number of materials including failure of quasi-brittle cement [41]. Experimental evidence of stochastic flaw-governed failure can be evaluated by comparing Weibull moduli between specimen types. If the process is governed by flaw quantity, then larger samples should have steeper Weibull moduli and smaller standard deviations. This is in agreement with our measurements (table 1).

3.5. Elastic properties of avian eggshells

The compression of hollow axisymmetric elastic membranes was first analysed by Timoshenko [36] and has been widely discussed in the literature. While analytical solutions are provided for some specific loading cases, the case of a point load is more complex. Such loading configuration induces a high concentration of stresses near the load points, and therefore, the resulting maximum tensile stress cannot be estimated by analytical methods due to singularities. Nonetheless, FEA methods can be applied.

Reissner [22] provides the following equation to obtain the Young's modulus, E, of a spheroidal shell under point load from a force–displacement curve:

$$E = \frac{F\sqrt{12(1-\nu^2)}}{8c(1-\rho)^2 y}, \tag{3.7}$$

Table 1. Average thickness, strength and Weibull modulus for different avian eggs.

bird/egg type	samples tested	thickness (μm)	strength (MPa)	Weibull modulus
quail	4	220	25.6	3.5
chicken (white-pullet)	6	440	30.9	3.6
chicken (white-AA)	20	350	28.8	7.0
chicken (hollow) (white-AA)	12	340	29.9	7.9
chicken (organic-AA)	10	410	25.6	6.3
chicken (white-jumbo)	18	400	18.3	2.0
goose	2	670	17.9	—
ostrich	4	2550	8.5	8.7

Table 2. Summary of reported values for the Young's modulus of chicken eggs.

author	test method	*E* (GPa)
Bain [42]	non-destructive distributed external load	26.3–34.1
Dhanoa *et al.* [43]	compressed circular ring	19.0
Lin *et al.* [44]	compressed circular ring	35.7
Manceau & Henderson [45]	distributed external load	17.7
Rehkugler [46]	compressed circular ring	10.5–20.7
Tung *et al.* [47]	compressed whole eggs	45.7–46.9
Kemps *et al.* [48]	vibration measurements	28.6
present study	flat plate compression tests	27.5

where F is the applied load, v is the Poisson ratio, c is the half-height of the spheroid, ρ is the thickness ratio ($\rho = R_{int}/R_{ext} = 1 - t/R_{ext}$) and y is the vertical displacement of the loaded point.

Applying equation (3.7) to experimental values (as the curve presented figure 5) along with FEA of point load experiments enabled the calculation of the Young's modulus of white-AA chicken eggs. An average value of 27.5 GPa was obtained, which is consistent with other reported measurements, summarized in table 2.

In order to determine Young's modulus for other types of tested eggshells, asymptotical slopes of force–displacement curves for distributed load tests were compared to an average slope for white chicken eggs. The ratio between slopes was then considered as a proportionality factor to multiply with the previously calculated value of E of chicken eggs (white-AA). Indeed, it was postulated that nonlinearity in the curves is introduced by the deformation of the rubber; hence the normalized slopes provide information on the elasticity of the eggshell. According to Hertz contact theory, a hollow sphere deforms linearly when in contact with a concave surface [49]; this was extended to our compression experiments on eggshells.

Calculated Young's moduli are presented figure 15. The results do not show a trend according to egg size, but highlight the fact that chicken white standard eggs are statistically the most rigid (Scheffé $p < 0.01$) as compared to all others, with the exception of jumbo eggs (Scheffé $p = 0.76$). Interestingly, organic chicken eggs, which are highly comparable in geometry, are

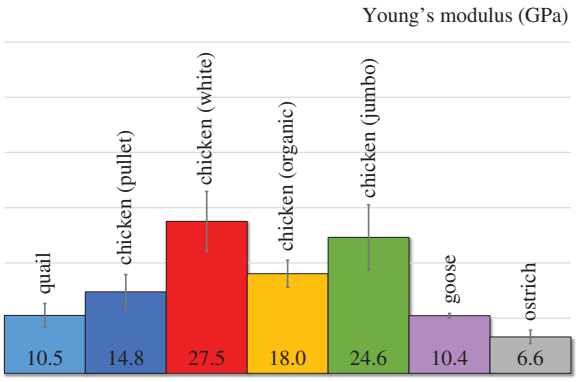

Figure 15. Young's moduli evaluated for eggshells. Results are ordered by egg size and error bars represent standard deviations. (Online version in colour.)

significantly more compliant. Curtis *et al.* [50] observed higher densities of organic content in brown eggs (more often encountered among organic or cage free eggs), which may contribute to their compliance and reduced brittleness.

An average Young's modulus of 6.6 GPa was found for ostrich eggs, which is in high contradiction with the 100 GPa value obtained by Nedomová *et al.* [26]. Nonetheless, the reported force–displacement curves for point load tests on ostrich eggs [26] were input into equation (3.7) and give a value of 6.5 GPa, which is remarkably close to the modulus calculated herein.

4. Conclusion

We have demonstrated that eggshells are excellent examples of technical ceramics developed by natural evolution. Subjected to loads focused at the pole of the egg (point loading), failure occurs by local fracture along the inner surface of the egg. The local deformation increases the contact area and multiple fracture events continue to occur without total egg failure, even to relatively large strains. On the other hand, as loading becomes dispersed (by using load-distributing pads) the failure mode shifts to tensile failure by axial splitting, followed by fracturing of the segments. Failure initiates at an angle offset from the distributed load, influenced by the overall geometry of the shell. This loading configuration facilitates the assessment of the ultimate tensile strength, although analytical methods fail to provide an exact estimate. The strength of eggshells decreases with increasing egg size, whereas the force required to break the egg

increases. The quantity and size of defects, in addition to protein content may have important consequences regarding the evolution of avian eggs. Resistance to compression and the amount of defects are closely related to the survivability and hatchability of the egg, but this topic is beyond the scope of the present work. The reduced strength of larger eggs can be justified from a microstructural perspective, taking into account an increased quantity and size of flaws for larger eggshells.

Data accessibility. All data will be shared upon request from the corresponding author, contacted by email at mameyers@ucsd.edu.

Authors' contributions. D.J.F. and M.A.M. initiated the project and performed early testing. S.D.R., E.N.H. and V.R.S. conducted mechanical testing. V.R.S. and E.N.H. performed SEM preparation and observation. A.P. performed FEA. A.P. and E.N.H. performed derivations and calculations. All authors contributed to the discussion and writing of the manuscript.

Competing interests. We have no competing interests.

Funding. This work was funded in full by the Multi-University Research Initiative grant no. AFOSR-FA9550-15-1-0009 from the Air Force Office of Scientific Research.

Acknowledgements. We gratefully acknowledge use of a Phantom high-speed camera provided by Prof. Vitali Nesterenko, and training for the camera by Andrew Marquez. We gratefully acknowledge Dr Bin Wang for assistance in the SEM. Valerie Sapp provided crucial statistical expertise in the treatment of our data. Prof. Po-Yu Chen, Prof. David Kisailus and Jerry Jung provided useful discussions regarding the project.

References

1. Rodriguez-Navarro A, Kalin O, Nys Y, Garcia-Ruiz J. 2002 Influence of the microstructure on the shell strength of eggs laid by hens of different ages. *Br. Poult. Sci.* **43**, 395–403. (doi:10.1080/00071660120103675)
2. Ahmed A, Rodríguez-Navarro AB, Vidal M, Gautron J, García-Ruiz JM, Nys Y. 2005 Changes in eggshell mechanical properties, crystallographic texture and in matrix proteins induced by moult in hens. *Br. Poult. Sci.* **46**, 268–279. (doi:10.1080/00071660500065425)
3. Hincke MT, Nys Y, Gautron J, Mann K, Rodriguez-Navarro AB, McKee MD. 2012 The eggshell: structure, composition and mineralization. *Front. Biosci.* **17**, 1266–1280. (doi:10.2741/3985)
4. Nys Y, Gautron J, Garcia-Ruiz JM, Hincke MT. 2004 Avian eggshell mineralization: biochemical and functional characterization of matrix proteins. *C. R. Palevol.* **3**, 549–562. (doi:10.1016/j.crpv.2004.08.002)
5. Hamilton R. 1986 The microstructure of the hen's egg shell—a short review. *Food Struct.* **5**, 13.
6. Rodriguez-Navarro A, Garcia-Ruiz JM. 2000 Model of textural development of layered crystal aggregates. *Eur. J. Mineral.* **12**, 609–614. (doi:10.1127/ejm/12/3/0609)
7. Arias JL, Fink DJ, Xiao S-Q, Heuer AH, Caplan AI. 1993 Biomineralization and eggshells: cell-mediated acellular compartments of mineralized extracellular matrix. *Int. Rev. Cytol.* **145**, 217–250. (doi:10.1016/S0074-7696(08)60428-3)
8. Tyler C. 1961 Studies on egg shells. XVI.—variations in shell thickness over different parts of the same shell. *J. Sci. Food Agric.* **12**, 459–470. (doi:10.1002/jsfa.2740120606)
9. Tyler C, Geake FH. 1961 Studies on egg shells. XV.—critical appraisal of various methods of assessing shell thickness. *J. Sci. Food Agric.* **12**, 281–289. (doi:10.1002/jsfa.2740120404)
10. Kerestes D, Boess B, Cosgrove A, Gleich H, Linonis K, Neal S. 2016 Chickens and Eggs. United States Department of Agriculture, National Agricultural Statistics Service. See http://usda.mannlib.cornell.edu/MannUsda/viewDocumentInfo.do?documentID=1028 (accessed 1 October 2016).
11. Hamilton RMJ, Hollands KG, Voisey PW, Grunder AA. 1979 Relationship between egg shell quality and shell breakage and factors that affect shell breakage in the field: a review. *Worlds Poult. Sci. J.* **35**, 177–190. (doi:10.1079/WPS19790014)
12. Roland D. 1977 The extent of uncollected eggs due to inadequate shell. *Poult. Sci.* **56**, 1517–1521. (doi:10.3382/ps.0561517)
13. Bureau of Labor Statistics, U.S. Department of Labor. *Consumer Price Index*, APU0000708111. [www.bls.gov/cpi/]. (Accessed 1 October 2016).
14. Ketelaere BD, Govaerts T, Coucke P, Dewil E, Visscher J, Decuypere E, Baerdemaeker JD. 2002 Measuring the eggshell strength of 6 different genetic strains of laying hens: techniques and comparisons. *Br. Poult. Sci.* **43**, 238–244. (doi:10.1080/00071660120121454)
15. Lin H, Mertens K, Kemps B, Govaerts T, De ketelaere B, De baerdemaeker J, Decuypere E, Buyse J. 2004 New approach of testing the effect of heat stress on eggshell quality: mechanical and material properties of eggshell and membrane. *Br. Poult. Sci.* **45**, 476–482. (doi:10.1080/00071660400001173)
16. Abanikannda O, Leigh A. 2007 Allometric relationships between composition and size of chicken table eggs. *Int. J. Poult. Sci.* **6**, 1–217. (doi:10.3923/ijps.2007.211.217)
17. Buchar J, Severa L, Simeonovová J. 2002 Determination of hen's eggshell elastic properties under quasistatic compression. In *Physical methods in agriculture* (eds J Blahovec, M Kutílek), pp. 157–165. New York, NY: Springer.
18. Trnka J, Buchar J, Severa L, Nedomová Š, Stoklasová P. 2012 Effect of loading rate on hen's eggshell mechanics. *J. Food Res.* **1**, 96. (doi:10.5539/jfr.v1n4p96)
19. Ar A, Rahn H, Paganelli CV. 1979 The avian egg: mass and strength. *Condor* **81**, 331–337. (doi:10.2307/1366955)
20. Macleod N, Bain MM, Hancock JW. 2006 The mechanics and mechanisms of failure of hens' eggs. *Int. J. Fract.* **142**, 29–41. (doi:10.1007/s10704-006-9018-5)
21. Bain MM. 1992 Eggshell strength: a relationship between the mechanism of failure and the ultrastructural organisation of the mammillary layer. *Br. Poult. Sci.* **33**, 303–319. (doi:10.1080/00071669208417469)
22. Reissner E. 1959 The edge effect in symmetric bending of shallow shells of revolution. *Commun. Pure Appl. Math.* **12**, 385–398. (doi:10.1002/cpa.3160120211)
23. Nedomová Š, Buchar J, Strnková J. 2014 Gooses eggshell strength at compressive loading. *Potravinarstvo* **8**, 54–61. (doi:10.5219/346)
24. Cooper RG, Lukaszewicz M, Horbanczuk JO. 2009 The ostrich (*Struthio camelus*) egg—a safety seat in the time vehicle. *Turk. J. Vet. Anim. Sci.* **33**, 77–80.
25. Nedomová Š, Buchar J. 2013 Ostrich eggs geometry. *Acta Univ. Agric. Silvic. Mendel. Brun.* **61**, 735–742. (doi:10.11118/actaun201361030735)
26. Nedomová Š, Buchar J, Strnková J. 2013 Mechanical behaviour of ostrich's eggshell at compression. *Acta Univ. Agric. Silvic. Mendel. Brun.* **61**, 729–734. (doi:10.11118/actaun201361030729)
27. Li D, Wong LNY. 2012 The Brazilian disc test for rock mechanics applications: review and new insights. *Rock Mech. Rock Eng.* **46**, 269–287. (doi:10.1007/s00603-012-0257-7)
28. Entwistle KM, Reddy TY. 1996 The fracture strength under internal pressure of the eggshell of the domestic fowl. *Proc. R. Soc. Lond. B* **263**, 433–438. (doi:10.1098/rspb.1996.0065)
29. Nedomová Š, Buchar J, Křivánek I. 2007 The effect of the egg's shape on the stress distribution in the eggshell at internal pressure loading. *Acta Univ. Agric. Silvic. Mendel. Brun.* **55**, 129–142. (doi:10.11118/actaun200755010129)
30. Trnka J, Nedomová Š, Kumbár V, Šustr M, Buchar J. 2016 A new approach to analyze the dynamic strength of eggs. *J. Biol. Phys.* **42**, 525–537. (doi:10.1007/s10867-016-9420-9)
31. Nedomová Š, Kumbár V, Trnka J, Buchar J. 2016 Effect of the loading rate on compressive properties of goose eggs. *J. Biol. Phys.* **42**, 223–233. (doi:10.1007/s10867-015-9403-2)
32. Sun CJ, Chen SR, Xu GY, Liu XM, Yang N. 2012 Global variation and uniformity of eggshell thickness for chicken eggs. *Poult. Sci.* **91**, 2718–2721. (doi:10.3382/ps.2012-02220)

33. Yan Y-Y, Sun C-J, Lian L, Zheng J-X, Xu G-Y, Yang N. 2014 Effect of uniformity of eggshell thickness on eggshell quality in chickens. *J. Poult. Sci*. **51**, 338–342. (doi:10.2141/jpsa.0130032)
34. Voisey PW, Hunt JR. 1969 Effect of compression speed on the behaviour of eggshells. *J. Agric. Eng. Res*. **14**, 40–46. (doi:10.1016/0021-8634(69)90065-1)
35. Billington DP. 1982 *Thin shell concrete structures*, 2nd edn. New York, NY: McGraw-Hill.
36. Timoshenko SP, Woinowsky-Krieger S. 1959 *Theory of plates and shells*, 2nd edn. New York, NY: McGraw-Hill.
37. Reissner E. 1946 Stresses and small displacements of shallow spherical shells. II. *J. Math. Phys*. **25**, 279–300. (doi:10.1002/sapm1946251279)
38. Fuenkajorn K, Klanphumeesri S. 2011 Laboratory determination of direct tensile strength and deformability of intact rocks. *Geotech. Test. J*. **34**, 1–6. (doi:10.1520/GTJ103134)
39. Meyers MA, Chawla KK. 2009 *Mechanical behavior of materials*, 2nd edn. Cambridge, UK: Cambridge University Press.
40. Taylor D, Walsh M, Cullen A, O'Reilly P. 2016 The fracture toughness of eggshell. *Acta Biomater*. **37**, 21–27. (doi:10.1016/j.actbio.2016.04.028)
41. Bazant Z, Novák D. 2003 Stochastic models for deformation and failure of quasibrittle structures: recent advances and new directions. In *Computational modelling of concrete structures*, pp. 583–598. Lisse, The Netherlands: Swets and Zeitlinger.
42. Bain MM. 1990 Eggshell strength: A mechanical/ultrastructural evaluation. PhD thesis, University of Glasgow, Glasgow, UK.
43. Dhanoa P, Puri V, Anantheswaran R. 1996 Thermal and mechanical properties of eggshell under different treatments. *Trans. ASAE* **39**, 999–1004. (doi:10.13031/2013.27588)
44. Lin J, Fajardo T, Puri V, Anantheswaran R, MacNeil J. 1993 Measurement of mechanical and thermal properties for eggshell quality determination. In *American Society of Agricultural Engineers Meeting* (*USA*), no. 936053. St Joseph, MI: ASABE.
45. Manceau J, Henderson J. 1970 Physical properties of eggshell. *Trans. ASAE* **13**, 436–439. (doi:10.13031/2013.38629)
46. Rehkugler G. 1963 Modulus of elasticity and ultimate strength of the hen's egg shell. *J. Agric. Eng. Res*. **8**, 352–354.
47. Tung MA, Staley LM, Richards JF. 1968 Studies on egg shell strength, shell stiffness, shell quantity, egg size and shape. *Br. Poult. Sci*. **9**, 221–229. (doi:10.1080/0007166680841 5713)
48. Kemps B, De Ketelaere B, Bamelis F, Govaerts T, Mertens K, Kamers B, Tona K, Decuypere E, De Baerdemaeker J. 2004 Development of a methodology for the calculation of Young's modulus of eggshell using vibration measurements. *Biosyst. Eng*. **89**, 215–221. (doi:10.1016/j.biosystemseng.2004.06.004)
49. Mansoor Baghaei S, Sadegh AM. 2011 Elastic spherical shell impacted with an elastic barrier: a closed form solution. *Int. J. Solids Struct*. **48**, 3257–3266. (doi:10.1016/j.ijsolstr.2011.07.016)
50. Curtis P, Gardner F, Mellor D. 1985 A comparison of selected quality and compositional characteristics of brown and white shell eggs. I. Shell quality. *Poult. Sci*. **64**, 297–301. (doi:10.3382/ps.0640297)